

# Experimental Investigation of Pore Structure Damage in Pulverized Coal: Implications for Methane Adsorption and Diffusion Characteristics

Kan Jin,<sup>†,‡,§</sup> Yuanping Cheng,<sup>\*,†,‡,§,||</sup> Qingquan Liu,<sup>†,‡,§</sup> Wei Zhao,<sup>†,‡,§</sup> Liang Wang,<sup>†,‡,§</sup> Fei Wang,<sup>†,‡,§</sup> and Dongmei Wu<sup>†,‡,§</sup>

<sup>†</sup>Key Laboratory of Coal Methane and Fire Control, Ministry of Education, China University of Mining and Technology, Xuzhou, Jiangsu 221116, China

<sup>‡</sup>National Engineering Research Center for Coal and Gas Control, China University of Mining and Technology, Xuzhou, Jiangsu 221116, China

<sup>§</sup>School of Safety Engineering, China University of Mining and Technology, Xuzhou, Jiangsu 221116, China

<sup>||</sup>School of Civil, Mining & Environmental Engineering, University of Wollongong, Wollongong, NSW 2522, Australia

**ABSTRACT:** To study the effect of pulverization on coal's pore structure and the implications for methane adsorption and diffusion properties, three kinds of high volatile bituminous coals were sampled and crushed into six kinds of particle sizes to conduct the experiments using a combination of proximate analysis, N<sub>2</sub> (77 K)/CO<sub>2</sub> (273 K) adsorption pore structure characterization, and high-pressure methane adsorption and diffusion properties determination. Results indicate that the pulverization process has no remarkable influence on the proximate properties of the coal, while the pore structures are evidently modified. The pulverization process significantly increases the specific surface area and pore volume (measured by N<sub>2</sub> adsorption) of the coal, which favors gas adsorption and diffusion. However, its effects on <2 nm micropore structure (measured by CO<sub>2</sub> adsorption) are variable. The high-pressure methane adsorption and diffusion tests demonstrate that the adsorption volume and diffusion quantities both increase with the decrease of coal particle size. The adsorption experiments also indicate that because of the complex adsorption mechanism, the high-pressure adsorption capacities of the coal are comprehensively influenced by the <2 nm micropore (measured by CO<sub>2</sub> adsorption) as well as the additional BET specific surface area and pore volume (diameter below 10 nm, measured by N<sub>2</sub> adsorption) that are generated during the pulverization process. Moreover, methane desorption experiments reveal the existence of coal rank-dependent extremity particle size, which can significantly affect the diffusion performance of methane within coal.

## 1. INTRODUCTION

Coal is a natural organic rock with complicated pore geometry and huge internal surface area,<sup>1–4</sup> which is also the source and reservoir for coalbed methane (CBM).<sup>5,6</sup> Affected by repeated geological tectonic motions,<sup>7</sup> the vast majority of the coal seams underground are always segmented by the extension of fractures or cleats<sup>8–10</sup> and extruded and broken by the plastic, ductile, or flowing deformation,<sup>11–13</sup> leading to a fragmentation or even pulverization of the coal mass. Moreover, mining activities, such as drilling, tunneling, blasting, etc., will also result in the fragmentation of coal.

Researchers in the coal industry have long been aware that the gas emission rate and the tendency of coal and gas outburst from a fragmented coal seam are quite different from those of an unpulverized coal.<sup>14</sup> Since the 1960s, to gain an understanding of the nature of the gas emission process, much work has been conducted on the gas adsorption and desorption properties of pulverized coal. Airey (1968)<sup>15</sup> measured and introduced an empirical formula to describe the methane release rate from seven sizes of coal (from <200 mesh to 0.25–0.5 in.), pointing out that if the coal particle exceeds a certain size (~6 mm), the continuous increase of the size almost does not affect the coal's diffusion coefficient. However, Bertard et al. (1970)<sup>16</sup> and Bielicki et al. (1972)<sup>17</sup> argued that corresponding to the coal's

natural fissuring network this certain size should not exceed 1 mm, and when the coal's particle size drops below 1 mm, the desorption rate would become inversely proportional to the square of the particle size. Nandi and Walker (1975)<sup>18</sup> observed similar effects of increasing diffusion parameters with decreasing particle size, considering that the pulverization of the coal particle would introduce additional macropores which would result in a positive influence on coal's diffusion rate. However, restricted by the experimental conditions, all of these contributions lacked detailed evaluation of the pore structures.

Recent studies demonstrate that the pore structures of the coal play a key role in various aspects of coal mine gas control and CBM exploitation, significantly influencing not only the gas storage or transportation in coal seams<sup>19,20</sup> but also the mechanisms of adsorption, diffusion, and desorption.<sup>12,21,22</sup> During the past two decades, with the development of the pore structure characterization technologies, great attention has been concentrated on the relationship between the pore structures and gas adsorption–diffusion–desorption properties.<sup>4,23–27</sup> Clarkson and Bustin (1999)<sup>19,20</sup> reviewed the conventional adsorption

Received: October 4, 2016

Revised: November 17, 2016

Published: November 18, 2016

Table 1. Locations, Petrographic Analyses, and Ranks of the Sampled Coals<sup>a</sup>

sample	sampling location	Ro (%)	petrographic composition (vol %)						coal rank
			macerals			minerals			
			V	I	L	CL	P	CA	
DL	no. 12 coal seam, Dalong Coal Mine, Tiefsa Coalfield, Liaoning Province	0.6406	92.39	3.36	0.89	2.81	0.45	0.10	high vol C
QN	no. 7 coal seam, Qinan Coal Mine, Huaibei Coalfield, Anhui Province	0.8134	83.49	13.71	1.35	0.85	0.32	0.28	high vol B
SL	no. 3 coal seam, Shuangliu Coal Mine, Hedong Coalfield, Shanxi Province	1.0754	95.95	1.88	0	1.55	0.62	0	high vol A

<sup>a</sup>Ro, vitrinite reflectance; V, vitrinite; I, inertinite; L, liptinite; CL, clay; P, pyrite; CA, carbonate; vol, volatile.

and porosimetry analysis methods used in the determination of coal's gas adsorption capacities and pore size distribution and developed a new model for matrix gas diffusion and adsorption. Lutynski and González González (2016)<sup>28</sup> investigated the high-pressure sorption characteristics of coal with different particle sizes, indicating that the particle size has an impact on the sorption isotherm, which was attributed to the increase of ash/inertinite content in fine fractions. Karacan and Mitchell (2003)<sup>29</sup> compared the interrelation among pore structures, macerals composition, and gas sorption rates, indicating that because of the nature of low microporosity, the sorption rates in vitrinite- and liptinite-abundant coals are low. Azmi et al. (2006)<sup>30</sup> studied the gas adsorption of coal samples with varying mean sizes and attributed the enhanced gas adsorption rate of the smaller particles to their larger surface area available for adsorption, but they did not provide any surface area data.

In addition, in other research areas, more and more attention also has been concentrated on the effects of the sample particle size. Slezak et al. (2010)<sup>31</sup> analyzed the behavior of particles of different sizes in coal gasification using a computational fluid dynamics simulation method. Yu et al. (2005)<sup>32</sup> studied the effect of coal particle size on the proximate composition and the combustion properties, indicating that finer coal particles exhibit higher reactivity. Versan Kök et al. (1998)<sup>33</sup> investigated the effect of particle size on coal pyrolysis, finding that as the particle size decreased the peak temperature of the sample increased slightly. Gore and Crowe (1989)<sup>34</sup> proposed a physical model to explain the variation of turbulent intensity caused by the addition of different sized particles. Zhao et al. (2016)<sup>35</sup> discussed the effects of coal powders' rapid gas desorption on coal and gas outburst based on the desorption experiments of coal particles with different sizes. Zhong et al. (2014)<sup>36</sup> investigated the effect of particle size on coal's strength parameters, indicating that the compressive strength and Young's modulus of coal particles increase as the specimen size decreases. All of the research mentioned above are all closely related to the differences of the physical chemistry characteristics (proximate parameter, density, pore structure, gas desorption property, etc.) in the coal with different particle sizes. Despite the fact that many results have been achieved, the effects of coal breakage on pore structure modification and its implications for gas adsorption and diffusion remain unclear. In this article, the impact of particle pulverization on coal's pore volume and specific surface area is systematically evaluated using the physisorption method. Additionally, the variations in proximate analysis parameters and gas adsorption and diffusion characteristics of the pulverized coals are also investigated to reveal the interrelation among the proximate parameters, pore structures, and the adsorption/diffusion properties and to provide basic experimental data support for other studies concerning samples with different particle sizes.

## 2. SAMPLING AND METHODS

**2.1. Sample Collection.** To study the effect of particle breakage on coal's proximate parameters, pore structure, and adsorption and diffusion properties, three kinds of coal were sampled from three main coal basins of China, representing different coal ranks from the high volatile C bituminous coal (DL sample) to the high volatile A bituminous coal (SL sample). The detailed sampling locations and basic parameters of these coal samples are listed in Table 1.

Once a coal sample was obtained, the sample was sealed and immediately sent to the laboratory. When the coal sample was received, we first checked and removed the waste rock in the sample. We then crushed the selected samples using a fully cleaned hammer breaker. Finally, we sieved these pulverized coals into our desired particle sizes using standard sieves and conducted further experiments. Considering the limitation of the physisorption instrument to the sample size, each sample was crushed and sieved into six kinds of particle size (1–3 mm, 0.5–1 mm, 0.25–0.5 mm, 0.2–0.25 mm, 0.074–0.2 mm, <0.074 mm).

**2.2. Experimental Methods.** To study the variations in physical parameters among the different grain size samples, proximate parameters, pore structures, and methane adsorption and diffusion properties of the coal samples were analyzed.

The proximate analyses of the samples followed ISO recommendations (ISO Standard 11722-1999 for moisture, ISO Standard 1171-1997 for ash, and ISO Standard 562-1998 for volatile matter and fixed carbon) and used a 5E-MAG6600 automatic proximate analyzer (Changsha Kaiyuan Instruments, China).

The pore structure, pore volume, and specific surface area (SSA) analyses of the samples were characterized by a physisorption method (N<sub>2</sub> and CO<sub>2</sub> as the probe molecule), using an Autosorb iQ<sub>2</sub> instrument (Quantachrome Instruments, United States). Before each test, the sample was outgassed for over 12 h under 130 °C and turbo molecular pump vacuum to completely remove the moisture, adsorbed gases, and other impurities inside the coal. With the coal sample maintained at liquid nitrogen temperature (77 K), N<sub>2</sub> adsorption isotherms were obtained at the relative pressure ( $P/P_0$ ) ranging from 0.001 to 0.995. The saturation pressure ( $P_0$ ) of the nitrogen at 77 K was measured by the instrument using a  $P_0$  cell. N<sub>2</sub>-based adsorption data acquired on pulverized coal particles were interpreted using Brunauer–Emmett–Teller (BET)<sup>37</sup> analysis for SSA and Barrett–Joyner–Halenda (BJH)<sup>38</sup> and density functional theory (DFT) analysis for pore size distribution (PSD).<sup>39,40</sup> The micropore volume and micropore SSA of the samples were determined by the CO<sub>2</sub> gas adsorption at 273 K for the relative pressure ranging from  $3 \times 10^{-5}$  to 0.0289. A saturation pressure of 26 200 Torr<sup>39</sup> ( $\approx 3.496$  MPa) was used for the measurement, and the CO<sub>2</sub> (273 K) adsorption data were interpreted using DFT methods.

The high-pressure methane adsorption isotherms were measured according to the MT/T 752-1997 Standard, using HCA high-pressure volumetric equipment (Chongqing Research Institute of CCTEG, China) based on the static volumetric theory described by Sing (1982).<sup>41</sup> Before the test, approximately 50 g of coal sample was weighed and placed in a vacuum drying oven. After drying under 100 °C/4 Pa for 2 h, the sample was cooled to room temperature and placed in the sample container for an evacuation under 4 Pa for 24 h at 60 °C. After the evacuation, the sample container was cooled to 30 °C and the dead space volume in the container was determined by helium gas. Then, a 2 h evacuation was applied to completely exhaust the residual helium. The methane adsorption isotherm was tested at 30 °C with a maximum gas pressure of 6 MPa by the volumetric method. The sample

Table 2. Proximate Analysis Results of the Pulverized Coal Samples<sup>a</sup>

particle size (mm)	moisture (wt %)			ash (wt %)			volatile matter (wt %)			fixed carbon (wt %)		
	DL	QN	SL	DL	QN	SL	DL	QN	SL	DL	QN	SL
1–3	5.23	1.49	0.69	7.72	19.18	2.05	7.72	19.18	2.05	48.88	51.15	69.70
0.5–1	5.70	1.60	0.76	7.07	19.86	1.73	7.07	19.86	1.73	49.46	51.30	69.94
0.25–0.5	5.54	1.57	0.78	7.67	19.30	2.53	7.67	19.30	2.53	48.78	51.04	69.38
0.2–0.25	5.75	1.65	0.95	6.03	18.31	1.99	6.03	18.31	1.99	49.29	51.28	69.85
0.074–0.2	5.59	1.48	0.91	5.58	18.66	2.19	5.58	18.66	2.19	50.38	50.52	69.63
<0.074	4.67	1.47	0.89	8.08	21.48	2.44	8.08	21.48	2.44	50.64	49.72	69.13

<sup>a</sup>Moisture on air-dry basis; ash on a dry basis; volatile matter on dry ashfree basis; fixed carbon on air-dry basis.

container was linked to a reference container with measured dead volume. From the pressure changes of the reference container, the amount of methane that entered the sample container could be obtained according to the SRK equation of state.<sup>42</sup> In the same way, the volume changes of free gas in the sample container could be obtained by the pressure changes when the adsorption was balanced. Finally, the adsorption volume can be calculated by subtracting the free volume from the entered methane volume.

The gas diffusion properties of the samples were characterized by a volumetric method-based gas desorption experiment reported by Zhao et al. (2016).<sup>35</sup> Before the test, about 50 g of the coal sample was placed into the sample container and suffered an evacuation under 4 Pa for 24 h at 60 °C, completely exhausting the impurities in the coal. After outgassing, the container was injected with methane and placed in a 30 °C water bath for gas adsorption. When equilibrium was achieved, the container was opened and then connected to the gas volume measuring cylinder; the volume of gas desorbed from the coal at different times was read and recorded from the cylinder.

### 3. RESULTS AND ANALYSIS

**3.1. Proximate Analyses.** The proximate analysis results of the coal samples with different particle size are shown in Table 2. With the coal rank rising from high volatile C (DL samples) to high volatile A (SL samples), the moisture and volatile contents of the coal show an obvious decrease while the content of fixed carbon increases, which is consistent with the literature.<sup>24,25,43</sup> However, the ash content of the coal exhibits no marked relationship with the coal ranks, which is mainly because the ash content of the coal is influenced by the sedimentary environment of the coal basin instead of coalification.<sup>44</sup>

For the same rank coal with various particle size, despite the slight fluctuation of the data, the moisture content of the sample shows no significant differences with the decrease of particle size. Similar regularities are also noticed in the content of the volatile matter and fixed carbon. In contrast, the ash content of the samples seems to be enriched in the smallest particle, especially for the QN samples, which is similar to the previous study by Cloke et al. (2002)<sup>45</sup> who analyzed the proximate properties of the coals with different grain sizes and found the highest ash content in the smallest grain size fractions. The phenomenon that ash content increases as the particle size decreases is mainly due to the mineral matter (calcite, kaolinite, quartz, smectite, etc.) occurring in the coal<sup>33</sup> (Figure 1). These minerals have extremely tiny size, and during the pulverization, the minerals will be peeled off from the coal surface and suffer further breakage. Because of their tiny size, it is much easier for these minerals to pass through the finer sieves and finally to be enriched in the smallest particle.

The variation in ash content is not so obvious, and the adsorption and diffusion properties of the coals can be hardly affected just by a slight increase of the ash content. In summary, the particle breakage process has no remarkable effects on the

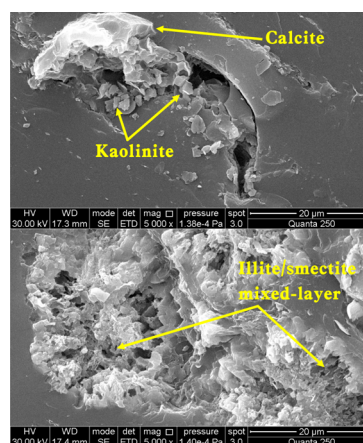
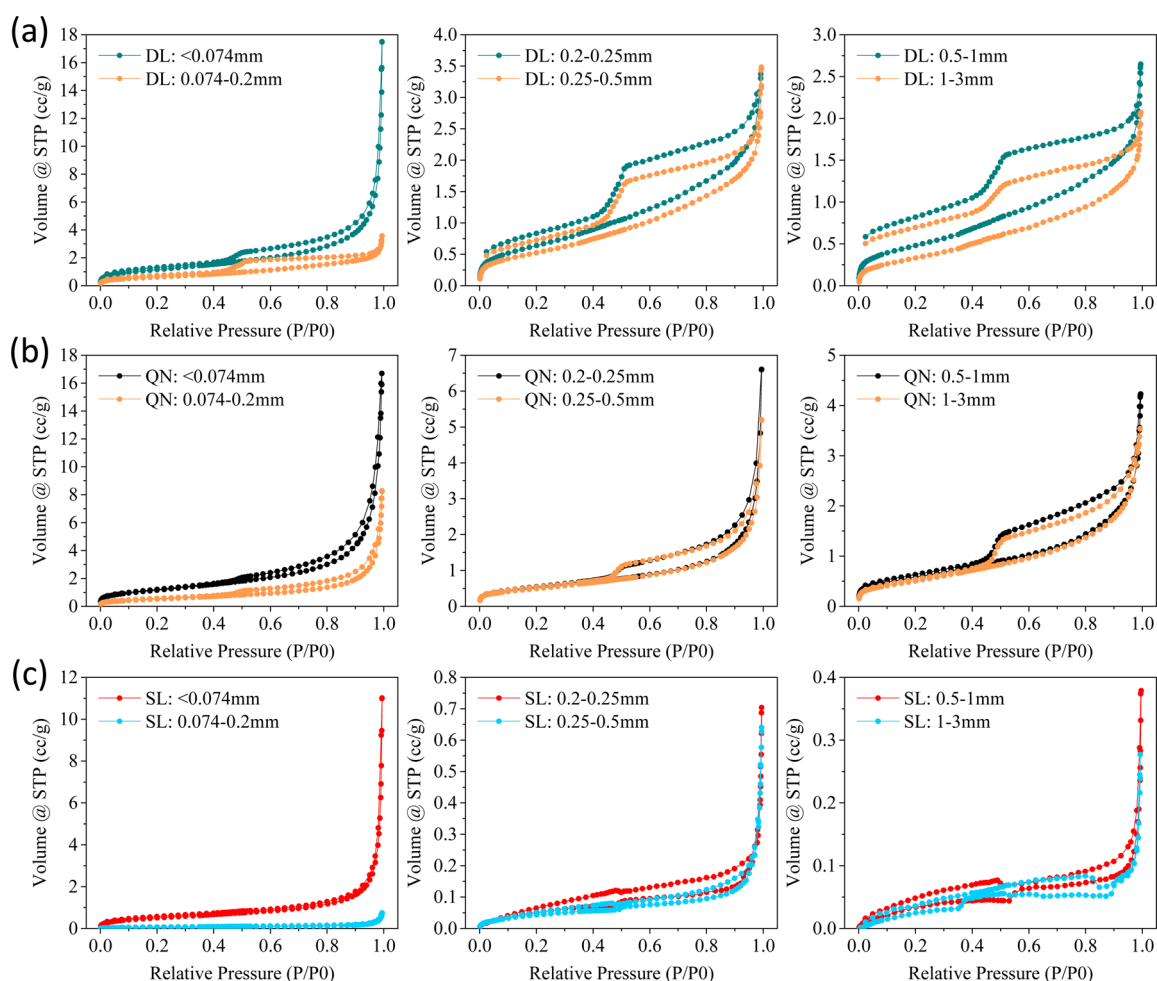


Figure 1. SEM photo showing the minerals in coal (DL sample).

proximate properties of the coals, and the often mentioned differences of adsorption and diffusion properties among various particle size samples may be attributed to the microstructural changes in coal's pore structure.

**3.2. Pore Structure Analyses Using N<sub>2</sub> Adsorption Method.** Studies on the pore structure of coals indicate the key pore size which mostly affects the adsorption and diffusion properties is located in the pores less than 10 nm and the pores ranging from 10 nm to hundreds of nanometers, respectively.<sup>22,46,47</sup> Therefore, the physisorption method applied here, which allows assessing a wide range of pore size ranging from 0.35 to 300 nm,<sup>48</sup> could provide the best analytical accuracy of the coal's pore structure.

**3.2.1. N<sub>2</sub> (77 K) Isotherms.** The N<sub>2</sub> (77 K) adsorption and desorption isotherms of the three rank coal samples with different particle size are shown in Figure 2. IUPAC<sup>49</sup> recommends the physisorption isotherms to be grouped into eight types, and for the coal samples tested in this article, the isotherms can be classified as a combination of type IV (a) and type II (at high  $P/P_0$ ) isotherms, indicating that the coals are one kind of micromeso–macroporous carbon-based adsorbents. The notable uptake of the isotherm at low  $P/P_0$  is related with the phenomenon of micropore filling, while point B, which is located at the start of the middle almost linear section of the isotherm, corresponds to the completion of monolayer coverage and the beginning of multilayer adsorption.<sup>50</sup> Then, followed by the pore condensation in the mesopores, the isotherm exhibits a rapid increase at high  $P/P_0$ . When  $P/P_0 \approx 1$ , because macropores whose pore size is larger than 300 nm exist in the coal,<sup>51</sup> the final saturation plateau as a typical feature of the type IV (a) isotherm does not appear but is replaced by an unlimited increasing trend, which is the feature of the type II isotherm, indicating the physisorption phenomenon on macroporous adsorbents.<sup>23,49</sup>



**Figure 2.**  $\text{N}_2$  (77 K) adsorption–desorption isotherms of the coal samples with various particle sizes: (a) DL coal samples, (b) QN coal samples, and (c) SL coal samples.

For the coal samples of the same rank, as the particle size decreases from 1–3 mm to  $<0.074$  mm, the maximum adsorption volume near  $P/P_0 \approx 1$  shows an evident increase and the adsorption branches of the isotherms become steeper, which represents larger pore volume and much more developed pore structures. The rough isotherms of the SL samples (Figure 2c) are related to the extremely small SSA values of the samples, which almost exceed the testing range of the instrument.

Despite the information gained from the types of physorption isotherms, the types of hysteresis loops are also closely related to the features of the pore structures and underlying adsorption and desorption mechanisms.<sup>52</sup> Referring to the IUPAC recommendations,<sup>49</sup> the hysteresis loops of the coal samples can be mainly classified as a type H4 loop, indicating that the coals are mainly composed by micropores, nonrigid aggregates of platelike particles, and are abundant in slit-shaped pores.<sup>2,49,53,54</sup>

In addition, for the DL samples, the lack of closure of the hysteresis loop is presented in Figure 2a. The generation of this phenomenon is mainly attributed to the swelling of the coal during the adsorption in micropores<sup>55</sup> and has been reported in several contributions,<sup>2,4,26,56,57</sup> especially for the high rank or low rank coals whose pore structures are much more complicated.

**3.2.2. Pore Size Distribution.** As a natural porous material, the pores in coal provide the space for methane occurrence and migration; thus, the pore size characteristics of the coal play a key

role in the performance of methane adsorption, diffusion, and penetration.<sup>19,22</sup> Generally accepted theory<sup>58,59</sup> in the coal industry and CBM exploitation field considers that the pores in coal whose size is  $<10$  nm provide the space for gas adsorption; the pores whose size is between 10 and 100 nm mainly constitute the space for gas diffusion; while the pores whose size is between 100 and 1000 nm constitute the slow penetration intervals. Considering the analysis ranges of the characterization methods and in order to fully reflect the PSDs of the pulverized coal, the recently developed DFT approach and the traditional BJH method are both introduced into the application so that a comprehensive analysis of the coals' pore structure from ca. 0.9 nm to ca. 400 nm can be conducted.

The controversy about the reliability of these two methods has been discussed for a long time. The generally accepted viewpoint indicates that the Kelvin equation-based BJH method may underestimate the pore size by up to 20–30% for narrow mesopores smaller than ca. 10 nm,<sup>48,54</sup> and this conclusion is also applicable to the analysis of the coal's pore structure (Figure 3). However, because the DFT approach only can provide the PSD below ca. 30 nm, the application of the traditional BJH method is still of great meaning in evaluating the PSD from tens to hundreds of nanometers, covering the crucial pore size affecting the diffusion properties of the coals.

In addition, considering the tensile strength effect (TSE)<sup>60</sup> observed in the isotherms (Figure 2), which is demonstrated as a

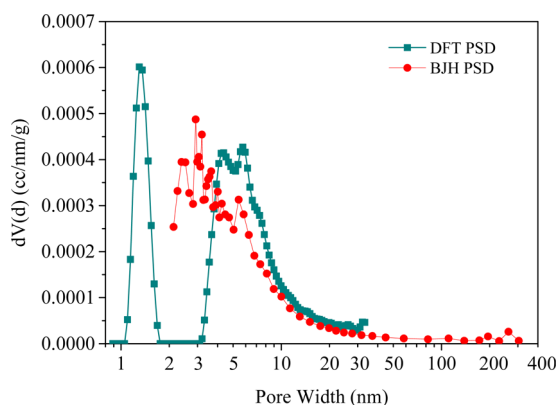


**Figure 3.** PSD comparison of the DFT approach with the traditional BJH method (DL sample with a particle size of 0.074–0.2 mm as an example).

forced closure of the desorption branch around  $P/P_0 = 0.45$  in the hysteresis loop, the PSD analyses of the samples were all based on the adsorption branches of the isotherms in order to avoid introducing extra peaks<sup>48</sup> (where actually no pores exist).

Compared to the widely used non-local density functional theory (NLDFT) method, the recently developed quenched solid density functional theory (QSDFT) allows the heterogeneity to be taken into account<sup>61</sup> and can significantly improve the reliability of the pore size analysis of microporous carbon materials.<sup>62</sup> Based on the QSDFT approach (kernel based on carbon, slit/cylinder pores), the PSDs of the samples are shown in Figure 4; the fitting errors of the samples are all below 1%. Additionally, the BJH method-based PSDs from 10 nm to ca. 400 nm is provided in Figure 4 as well.

The PSDs of the coal samples mostly exhibit a bimodal feature, one of the peaks located between 1 and 2 nm and the other between 4 and 5 nm, except for the samples whose particle size is

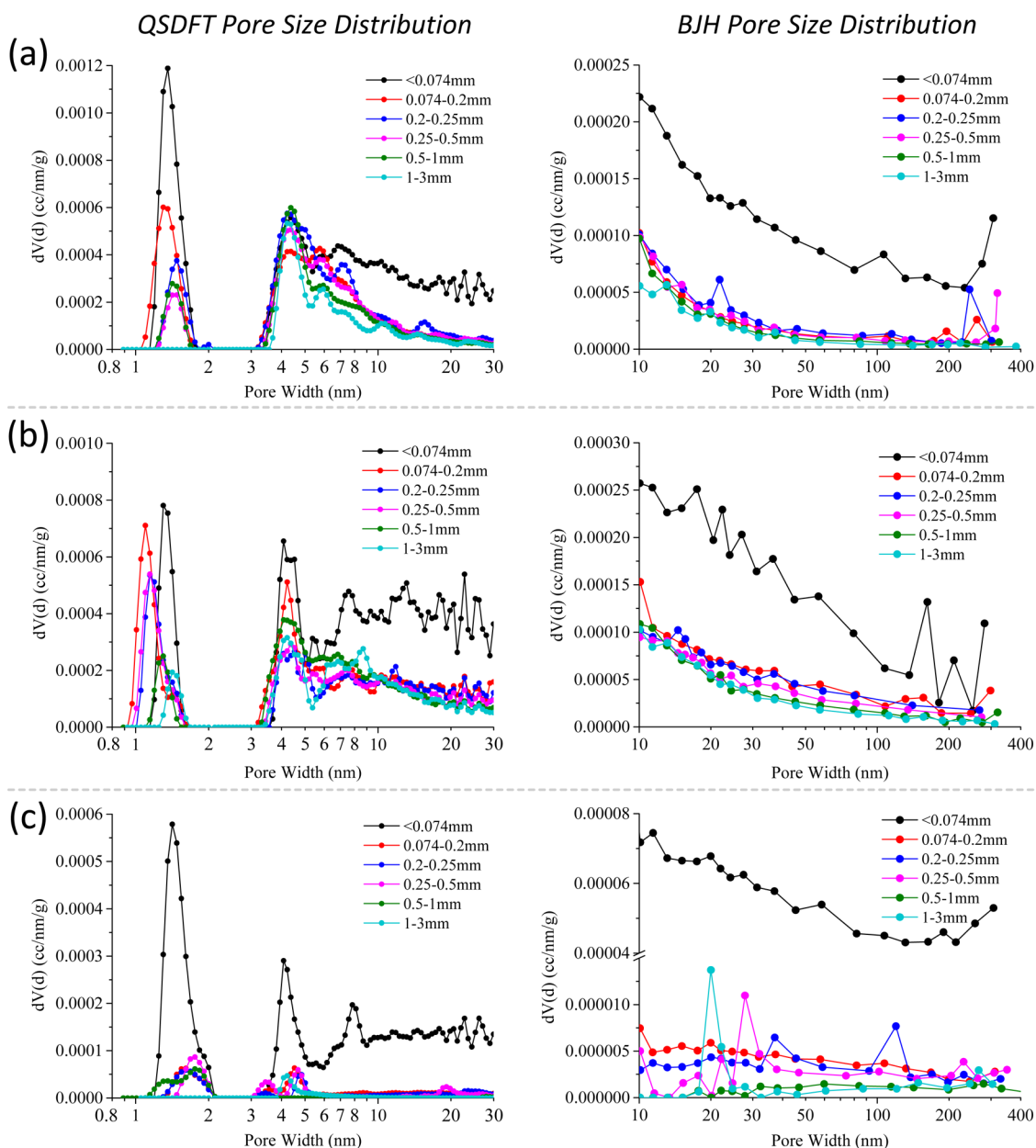


**Figure 4.** Pore size distribution of the coal samples with various particle sizes: (a) DL coal samples, (b) QN coal samples, and (c) SL coal samples.

Table 3. Specific Surface Area and Pore Volume of the Pulverized Coal Samples<sup>a</sup>

particle size (mm)	DL samples			QN samples			SL samples		
	BET SSA (m <sup>2</sup> /g)	pore volume (×10 <sup>-3</sup> cc/g)		BET SSA (m <sup>2</sup> /g)	pore volume (×10 <sup>-3</sup> cc/g)		BET SSA (m <sup>2</sup> /g)	pore volume (×10 <sup>-3</sup> cc/g)	
		PW < 10 nm	PW > 10 nm		PW < 10 nm	PW > 10 nm		PW < 10 nm	PW > 10 nm
1–3	1.323	1.266	1.931	1.819	1.299	6.722	0.055	0.036	0.530
0.5–1	1.806	1.738	2.366	1.841	1.306	7.759	0.110	0.049	0.452
0.25–0.5	1.997	1.956	3.413	1.952	1.309	8.780	0.191	0.086	0.915
0.2–0.25	2.283	2.114	3.408	1.977	1.634	11.865	0.254	0.118	1.159
0.074–0.2	2.657	2.417	4.199	2.158	1.756	13.797	0.309	0.181	1.508
<0.074	4.241	3.089	24.056	4.370	2.745	22.920	1.838	1.088	15.875

<sup>a</sup>SSA, specific surface area; PW, pore width.

<0.074 nm. The pore volume of the samples increase with the decrease of particle size. However, for the samples whose particle size is <0.074 nm, the pore volume of which exhibits an impressive step up, while the PSDs of which show the characteristics of multipeaks and a much smoother distribution of pores from ca. 7.5 nm to ca. 30 nm. Further observation of the peaks indicates that with the particle size decreasing, the mode diameter (<10 nm) of the sample almost remains the same while the incremental pore volume (dV(d)) shows an evident increase.

With the combined PSD analyses based on QSDFT and BJH methods, the conclusion can be drawn that the breakage of the coal significantly increases the pore volume of the pulverized coal particles, which will lead to a larger adsorption capacity and better diffusion properties especially for the particles with smaller grain size.

**3.2.3. Pore Volume and SSA.** To quantitatively evaluate the influence of pulverization on the detailed pore structure parameters, the BET SSA and pore volume of the pulverized coal samples are calculated and listed in Table 3. What should be noticed is that the pore volume whose pore widths are <10 nm are acquired by the QSDFT method and the pore volume whose pore widths are >10 nm are acquired by the BJH method.

With the increase of pulverization, the BET SSA and the pore volume of the coal samples all exhibit an increasing trend with the decrease of the particle size. The BET SSA values of the samples whose particle size is <0.074 mm are 3.21 (DL samples), 2.40 (QN samples), and 33.42 (SL samples) times greater than that of 1–3 mm. The pore volumes (pore widths < 10 nm) of the samples whose particle size is <0.074 mm are 2.44 (DL samples), 2.11 (QN samples), and 30.22 (SL samples) times greater than that of 1–3 mm. In summary, the pulverization of the coal particles remarkably raises the SSA and the pore volume (pore widths < 10 nm) of the coal, which favors gas adsorption.

Moreover, pore volumes (pore widths > 10 nm) of the coals are also obviously modified along with the breakage process. The pore volumes (pore widths > 10 nm) of the samples whose particle size is <0.074 mm are 12.46 (DL samples), 3.41 (QN samples), and 29.95 (SL samples) times greater than that of 1–3 mm. The percentage of the pores whose widths are >10 nm in the total pore volume is also evidently changed, especially for DL samples, whose ratio of the pore volume (pore widths > 10 nm) changed from 60.40% to 88.62%, and for the others this ratio is nearly 10%. This type of pore structure which is abundant in mesopores favors gas diffusion.

Additionally, when the coal particles are pulverized to the size <0.074 mm, the values of the BET SSA and the pore volume both exhibit a sudden step up compared to the change rule of larger particles, especially for SL samples whose BET SSA and pore volume of the particles <0.074 mm are nearly 30 times higher

that of the 1–3 mm samples, while the 0.074–0.2 mm particles are only 2.85–5.62 times greater than that of the 1–3 mm samples. The sudden increase of the SSA and pore volume with the coal pulverization indicates that a critical particle size may exist. When the coals are pulverized to the size below a certain value, the pore structure modification of the coal will transform from a partial damage to a comprehensive destruction, leading to a radical change of the gas adsorption and diffusion properties.

The increasing of pore volume may relate to the additional pores generated in the pulverization process<sup>63</sup> and may also relate to the more intergranular pores in the stacked particles when the experiments were conducted. In an attempt to evaluate the percentage of additional generated pores in the pulverized samples, the <0.074 mm particles of DL samples were compacted to tablets of 3 mm diameter by a hydraulic press at 2 t pressure, aiming to completely eliminate the intergranular pores among the particles. Then N<sub>2</sub> (77 K) isotherms of the <0.074 mm powder, compacted tablets, and 1–3 mm samples were measured. The results (Figure 5) show that the BET SSA of

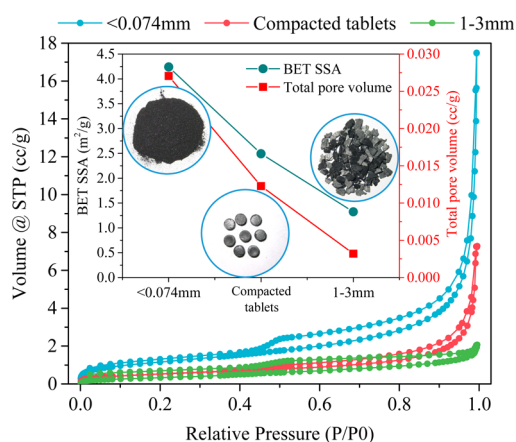


Figure 5. Effects of powder compaction on N<sub>2</sub> (77 K) isotherms, BET SSA, and total pore volume.

the tablets is 58.76% of the <0.074 mm powder and that the total pore volume reaches 45.34%. The BET SSA and total pore volume of the tablets are 1.88 and 3.83 times greater than that of the 1–3 mm samples, respectively. Therefore, the pulverization process indeed generates pores in coal, and these additional generated pores occupy at least half of the total SSA and pore volume in the sample. What should be noted is that this result is a bit rough, because the pressure generated by the hydraulic press is too large when compared to results reported by Li et al.

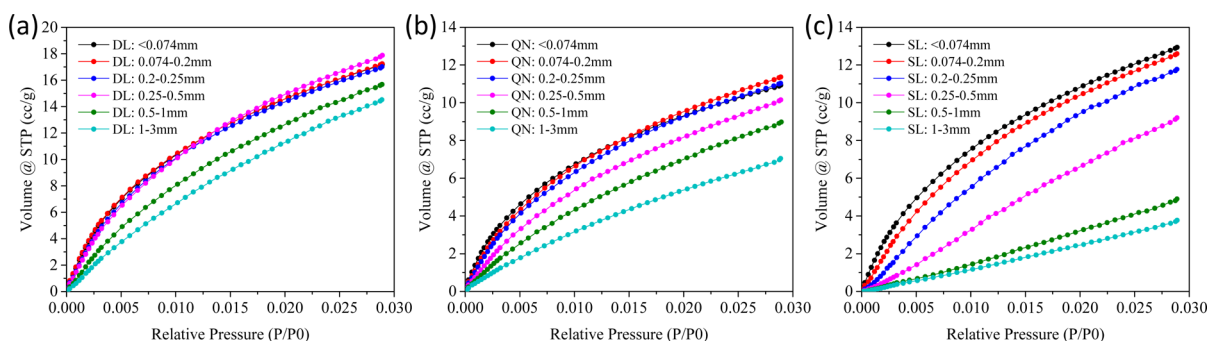


Figure 6. CO<sub>2</sub> (273 K) adsorption isotherms of the coal samples with various particle sizes: (a) DL samples, (b) QN samples, and (c) SL samples.

Table 4. Micropore Volume and Micropore Surface Area of the Pulverized Coal Samples

particle size (mm)	DL samples		QN samples		SL samples	
	micropore volume (cc/g)	micropore surface area (m <sup>2</sup> /g)	micropore volume (cc/g)	micropore surface area (m <sup>2</sup> /g)	micropore volume (cc/g)	micropore surface area (m <sup>2</sup> /g)
1–3	0.055	153.62	0.028	76.56	0.016	40.54
0.5–1	0.057	167.19	0.032	93.41	0.021	53.15
0.25–0.5	0.059	187.06	0.037	109.64	0.037	96.57
0.2–0.25	0.057	179.85	0.037	115.68	0.041	119.57
0.074–0.2	0.058	184.16	0.038	119.96	0.044	133.42
<0.074	0.054	161.44	0.035	115.16	0.045	139.29

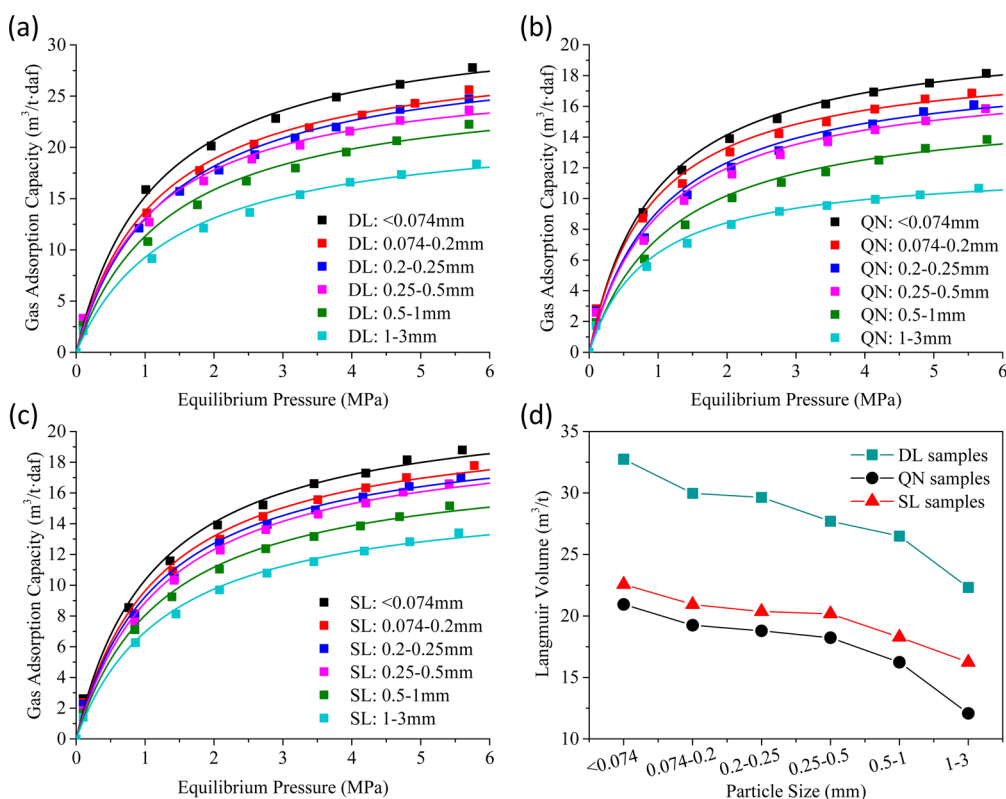
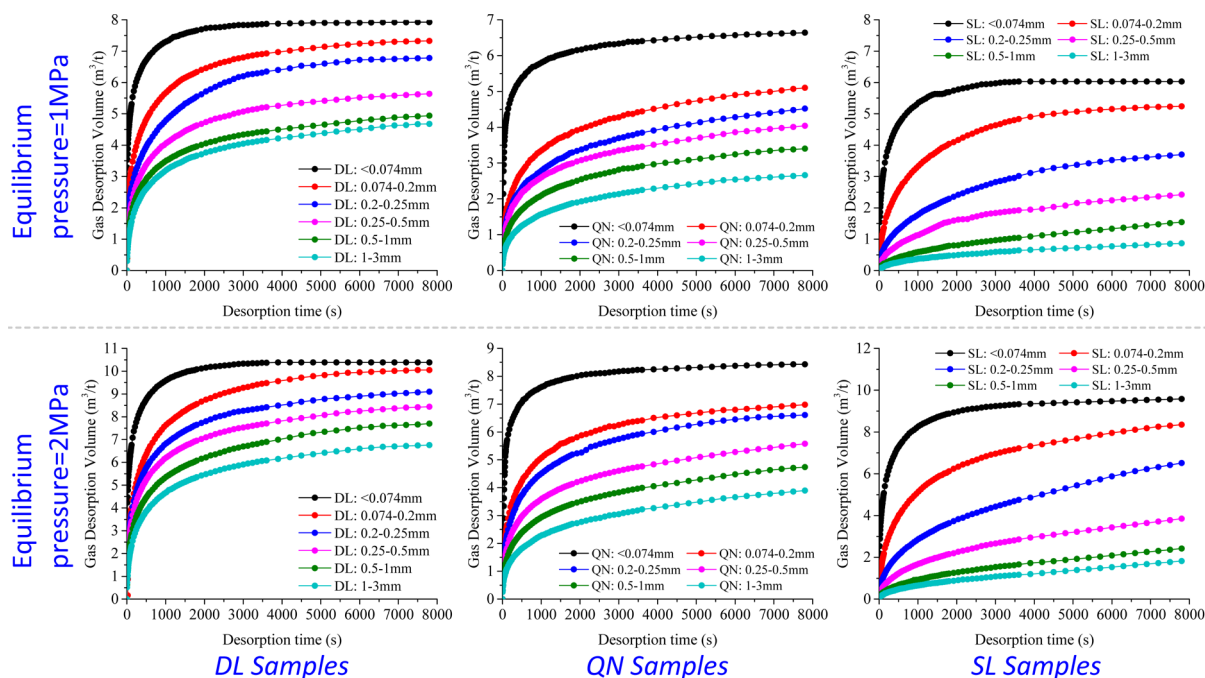


Figure 7. Methane adsorption isotherms of DL (a), QN (b) and SL (c) coal samples under 30 °C and the Langmuir volume ( $V_L$ ) variation of the samples (d).

(1999),<sup>64</sup> and the pore structure of the coal may be compacted to some extent as well; thus, further study is required.

**3.3. Micropore Analyses Using CO<sub>2</sub> Adsorption Method.** Micropore analyses of microporous materials have mainly been performed by nitrogen adsorption at 77 K. However, because of the slow diffusion rate of N<sub>2</sub> at 77 K and the diameter of N<sub>2</sub> molecule, this method is not satisfactory with

regard to a quantitative assessment of the microporosity, especially in the range of ultramicro pores (pore widths <0.7 nm).<sup>39</sup> Moreover, because of the much larger specific interactions for CO<sub>2</sub> than for N<sub>2</sub>, the differences in the coal micropore volume and surface area measured with these two gases are huge. The SSAs of coals measured by CO<sub>2</sub> often give the values of the order of several hundred square meters per



**Figure 8.** Methane desorption curves of the coal samples under different equilibrium pressures.

gram,<sup>65</sup> while SSAs obtained from N<sub>2</sub> are extremely small (see Table 3).

CO<sub>2</sub> (273 K) adsorption isotherms measured from differently sized samples are illustrated in Figure 6; CO<sub>2</sub> micropore volume and surface area obtained from the samples are given in Table 4. With the pulverization, the micropore volume and micropore surface area of the samples exhibit different variation characteristic. For DL and QN samples, both micropore volume and micropore surface area increase at first and then decrease, which is consistent with some previous studies,<sup>66</sup> indicating that the micropore structure in the coal suffered first from being generated or exposed (for closed pores) and then were ruined. However, the SL samples demonstrate different changing characteristics which exhibit a monotonic increasing regularity. In addition, with the rising of coal rank (from DL to SL), the magnitude of increase in micropore volume/surface area becomes much more obvious. The various performances of micropore volume and micropore surface area changing with the coal ranks indicate that with the rising of coal rank the physical structure as well as the coal matrix scale may undergo a vast modification.

**3.4. High-Pressure Methane Adsorption Characteristics.** The methane adsorption isotherms of the coal samples are shown in Figure 7a–c. To eliminate the effect of varying moisture and ash content in the samples, all of the data were calculated on a dry, ash-free basis. Moreover, it should be noted that the amount of adsorbed methane which was directly obtained from the experiments was a Gibbs surface excess (GSE) amount. The GSE amount neglects the volume occupied by the adsorbed gas at each equilibrium pressure step when calculating the amount of free gas,<sup>67</sup> resulting in the difference between GSE amount and the absolute adsorption, especially when the equilibrium pressures get higher. To calibrate this, the following equation is used.<sup>68</sup>

$$V_{\text{abs}} = \frac{V_{\text{Gibbs}}}{1 - \frac{\rho_{\text{gas}}}{\rho_{\text{ads}}}} \quad (1)$$

where  $V_{\text{abs}}$  and  $V_{\text{Gibbs}}$  are the absolute and Gibbs sorption, respectively, and  $\rho_{\text{gas}}$  and  $\rho_{\text{ads}}$  are gas densities in gaseous and adsorbed phases, respectively. The phase density for adsorbed methane ( $\rho_{\text{ads}}$ ) used to calculate the absolute adsorption is 0.421 g/cm<sup>3</sup>.<sup>69</sup>

The adsorption isotherm data were modeled to the Langmuir equation<sup>70</sup> because of its long and wide use in the coal science and industry field.<sup>68,71</sup>

$$V = \frac{V_L p}{P_L + p} \quad (2)$$

where  $V$  is the volume of adsorbed gas (m<sup>3</sup>/t);  $V_L$  is the Langmuir volume (m<sup>3</sup>/t), which is the maximum sorption capacity of the adsorbent based on monolayer adsorption;  $P_L$  is the Langmuir pressure (MPa), which is the pressure at which the total volume adsorbed ( $V$ ) is equal to one-half of the Langmuir volume ( $V_L$ ); and  $p$  is the equilibrium pressure (MPa).

It has been widely accepted that the methane adsorption capacities of the coal are closely related to the micropore structures, especially for the micropore whose diameter is less than 2 nm.<sup>6</sup> From Table 4 we know that the micropore volume of DL samples is 1.53–1.96 times greater than that of QN samples and 1.2–3.44 times greater than that of SL samples, and the  $V_L$  values of the samples (Figure 7d) are generally consistent with the CO<sub>2</sub> (273 k) micropore measurement results.

However, there are still some differences between the micropore results and the high-pressure methane adsorption characteristics. The adsorption isotherms (Figure 7a–c) indicate that with the pulverization, the methane adsorption volume of one certain rank coal increases with the decreasing grain size at the same equilibrium pressure. In addition, the Langmuir volumes of the samples (Figure 7d) show similar tendency; the  $V_L$  values of the samples whose particle size is <0.074 mm are 1.41–1.71 times greater than that of 1–3 mm samples. However, the micropore analyses (Section 3.3) indicate that for DL and QN samples, both micropore volume and surface area show a trend that first increases and then decreases. This phenomenon

may be explained by the pulverization-generated additional BET SSA and pore volume whose diameter is below 10 nm (measured by N<sub>2</sub> (77 K) adsorption, refer to Table 3), which along with the <2 nm micropore (measured by CO<sub>2</sub> (273 K) adsorption) comprehensively affect the high-pressure adsorption properties of the samples and result in the changing trend illustrated in Figure 7d.

**3.5. Methane Diffusion Properties.** To evaluate the effects of particle pulverization on coal's gas diffusion properties, methane desorption experiments of the coal samples with various particle sizes were conducted under two equilibrium pressures (1 and 2 MPa). The results (Figure 8) indicate the following:

(1) For almost all of the samples the initial rate of methane release is very large, and the smallest particle demonstrates the largest initial rate. With the increase of time, the methane release rate subsequently falls off progressively, and the rate of attenuation depends on the particle size of the coal as well as the desorption time.

(2) In the initial stage of the experiments (time < 1000 s), the smallest sample exhibits the fastest desorption rate and the slowest attenuation rate. The total methane desorption volume reaches its ultimate value after about 2000 s. After that, the methane release rate of the smallest sample decreases extremely rapid and finally reaches near zero. However, for larger particles, the initial methane release rate and the attenuation rate are much smaller. These samples continue to release methane after 8000 s when the experiments were terminated.

(3) The total desorption volumes of the coal (Figure 9) seem to have some connections with the pore structure parameters.

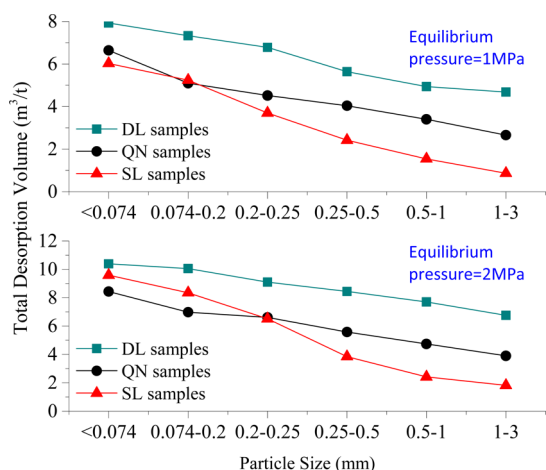


Figure 9. Total desorption volume of the coal samples (130 min).

Generally, with the most developed pore system, the DL samples give the largest desorption amount, while the SL samples have desorption volume similar to that of the QN samples in the smallest particle but suffered a much more obvious decrease when the sample size gets larger, which is consistent with the changing trend of pore volume and SSA.

## 4. DISCUSSION

**4.1. Pore Structures and Methane Adsorption.** The gas adsorption process of the coal can be divided into three steps:<sup>72</sup>

- (1) Gas molecules diffuse through the external coal surface layer.
- (2) Gas molecules pass through the internal pores.
- (3) Gas molecules are adsorbed by the pore wall. Previous research suggests that the pore structures of the coal have a significant

effect on the gas adsorption characteristics.<sup>12,19,21,22</sup> From the experimental results demonstrated in Results and Analysis, we find that the pulverization process does modify the coal's pore structures. However, despite the fact that many research results have been achieved, the mechanisms behind these results remain controversial.

Because the CO<sub>2</sub>-based micropore analysis results (section 3.2) do not give the conclusive evidence that is consistent with the high-pressure methane adsorption experiments, it is reasonable to presume that the pulverization-generated additional BET SSA and pore volume whose diameter is below 10 nm also have effects on high-pressure adsorption properties of the samples (many studies treat the pores in coal with diameter less than 10 nm all as micropores and consider that these pores also provide the adsorption capacities of the coal<sup>58,59,73</sup>). From section 3.2, N<sub>2</sub> (77 K) based experimental results have demonstrated that the pulverized coal has large increased SSA and pore volume, which means that extra pores have been introduced into the coal or the original closed pores have been penetrated, leading to a higher adsorption capacity and a faster equilibration period. A comparison of the pore structure parameters (SSA, pore volume) of the pulverized coals to their  $V_L$  values is illustrated in Figure 10. The BET SSA and the pore

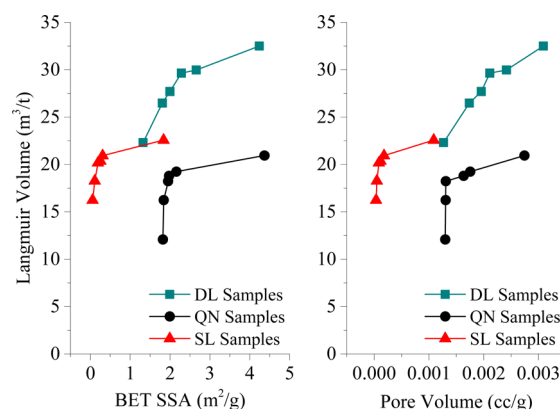


Figure 10. Correlation between pore structure parameters and the Langmuir volume.

volume (<10 nm pores) of the coals both exhibit increasing trend with the decrease of the coal particles, but no obvious relationship between the  $V_L$  values and the pore structure parameters can be detected. This phenomenon may be related to the pore structure characterization method and the mechanism of gas storage in the coals.

Moreover, with the increase of the SSA and pore volume, the  $V_L$  curves show a rapid growth in the initial stage and then bend to a much lower growth rate, indicating that a maximum value of the  $V_L$  for a certain coal may exist, namely, when the coal is pulverized into a critical size, the pore structure of the coal will be completely ruined and the internal surface of the coal can be entirely exposed.

**4.2. Pore Structures and Methane Diffusion.** Commonly, gas transport within the coal matrix is assumed to be concentration gradient driven diffusion and to occur in two stages:<sup>74,75</sup> (1) gas desorption from internal coal surface and (2) diffusion through the matrix and pore systems. For most coals, the first stage is sufficiently fast to be nearly negligible. Therefore, the mean width and connectivity of the pore systems and the length of gas diffusion path are of great importance in controlling

the diffusion process, which is also known as the extremity particle size<sup>76</sup> or the matrix size.<sup>35</sup> The extremity particle size represents the particle size at which the seepage system of the coal completely disappears,<sup>35</sup> and it is believed that only when the particles are grinded into a size below the extremity particle size will the gas diffusion properties of the coal particle result in a significant modification.

From Figure 8, the extremity particle size can be easily found in QN and SL samples, which divides the whole desorption stage into the rapid gas desorption stage and the normal or slow desorption stage. In the normal or slow desorption stage, the damage generated by the particle breakage has little influence on the matrix of the coal. Thus, the whole transport of gas through the porous system is not markedly changed. When the particle size decreases to a certain value below the matrix size (0.074 mm for QN samples and 0.2 mm for SL samples), the seepage system disappears and a great number of closed pores will be opened as well as many new generated pores, which finally exhibit a completely different diffusion regularity. However, the experimental data also indicate that the coal matrix scale may change with the variation of coal rank.

**4.3. Characterization Method for Pulverized Coal's Pore Structure.** With the development of the scientific technologies, more and more methods and instruments have been used to characterize the pore structure of the porous materials.<sup>77,78</sup> A summary of the methods and their ranges of application have been provided by Zhao et al. (2014)<sup>79</sup> as shown in Figure 11. Among them, the physisorption and mercury

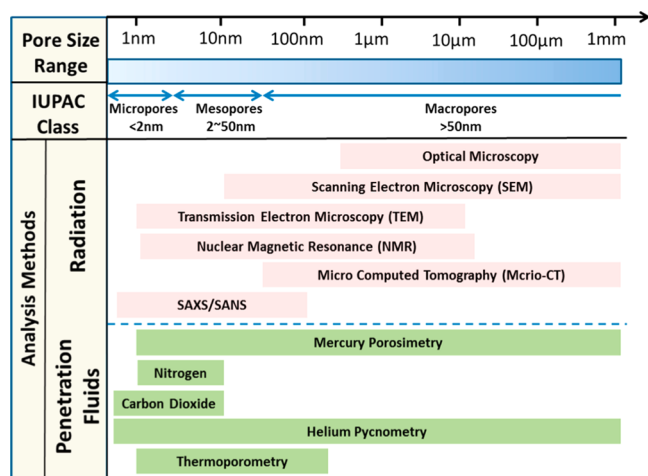


Figure 11. Methods used to estimate porosity and pore size distribution in coals or rocks. Reprinted from ref 79. Copyright 2014 American Chemical Society.

intrusion porosimetry method (MIP) are the most widely used technologies for the textural characterization of porous materials.<sup>39,80</sup> However, to accurately characterize the pore structure of the pulverized coal, some points need to be noticed.

Thommes (2010)<sup>54</sup> suggested that N<sub>2</sub> (77 K) adsorption is not satisfactory in the quantitative assessment of the microporosity, especially in the ultramicropores whose pore widths are <0.7 nm. Amarasekera et al. (1995)<sup>65</sup> and Ottiger et al. (2008)<sup>81</sup> indicated that gases like CO<sub>2</sub> and CH<sub>4</sub> not only adsorb on the coal surface but also dissolve into its structure, and their abilities to transport through the solid coal matrix will result in reaching all the pores in the coal, including those isolated ones regarded as not having surface openings. Therefore, the actual internal SSA

and pore volume of the coal for methane adsorption will be much larger than that measured by N<sub>2</sub> (77 K) adsorption method, and the CO<sub>2</sub> adsorption method which fully satisfies the micropore analysis demand is thereby recommended to be used so that a comprehensive analysis of the micropore structure of the coal can be achieved.

Moreover, as mentioned above, because of the limitation of the physisorption method, the best analytical accuracy of this method ranges from 0.35 to 300 nm.<sup>48</sup> Thus, for the macropore whose size is larger than 300 nm, the application of the MIP method is a wise selection.<sup>46</sup> However, challenges arise when using the MIP method to characterize the pore structure of pulverized coal. Figure 12 shows our attempt to characterize the

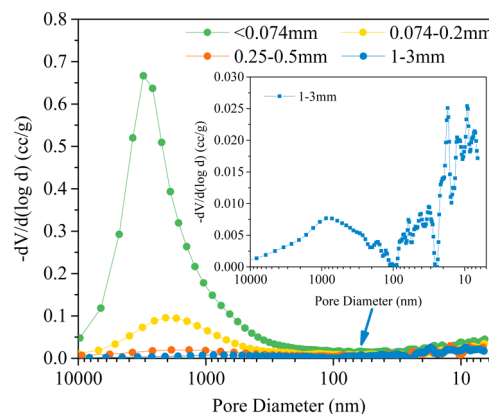


Figure 12. PSDs of differently sized samples based on MIP method.

pulverized coal using MIP method; the results indicate that while the 1–3 mm sized sample shows a pore size distribution curve typical of that illustrated in the literature, the PSD curves of the smaller samples exhibit significant differences. Especially for the <0.074 mm sample, the pore volume whose pore size is between 500 and 10000 nm is much greater than that in samples of other sizes. The reason may be attributed to the large amount of interparticle pores. The smaller sample contains many more coal particles with similar total mass, and some of these interparticle pores may have similar or even smaller size than the coal particle themselves. Therefore, while using the MIP method to characterize the pore structure, these interparticle pores will lead to an overestimated pore volume especially for the smaller sized samples. To solve this problem, the thinking provided by Li et al. (1999)<sup>64</sup> may be a good choice, which tries to eliminate the interparticle pores by compacting the powder into tablets. However, determining the critical pressure which can eliminate the interparticle pores without damaging the macropores requires vast work and further studies.

## 5. CONCLUSIONS

(1) Proximate analyses indicate that despite the slight enrichment tendency of the ash content in the smallest particle, the pulverization process has no remarkable effects on the proximate properties of the coals. The enrichment of the ash in the smallest grain size fractions is mainly due to the tiny mineral matter occurring in coal and peeled off during the breakage. Therefore, the differences of adsorption and diffusion properties among samples of various particle sizes may be attributed to the microstructural modification in the pore structures after the breakage of coal.

(2) The  $N_2$  (77 K) adsorption experiments demonstrate that with the pulverization of the coal particles, the BET SSA and the pore volume both increase with the decrease of grain size, while the mode pore size shows no significant change. The increase of SSA and pore volume may relate to the additional pores generated during the pulverization process and also relate to more intergranular pores occurring in the stacked particles. A rough evaluation indicates that the additional generated pores occupy at least half of the total SSA and pore volume in the sample. Additionally, when the coal particles are pulverized to the size  $<0.074$  mm, the BET SSA and the pore volume both exhibit a sudden step up when compared to the change rule of larger particles. The sudden increase may indicate the existence of the critical particle size, and when the coals are pulverized below this size, the pore structure modification will transform from a partial damage to a comprehensive destruction, leading to a radical change of the gas adsorption and diffusion properties.

(3)  $CO_2$  (273 K) micropore analyses indicate that the effects of pulverization on micropore volume and micropore surface area are variable. For DL and QN samples, both micropore volume and micropore surface area increase at first and then decrease. However, the SL samples exhibit a monotonic increasing regularity with the rising of breakage degree. The various performances of micropore structures indicate that there exist great differences in the physical structure and the coal matrix scale among various rank coals.

(4) The high-pressure methane adsorption and diffusion experiments demonstrate that the gas adsorption volume and diffusion quantities both increase with the decrease of the coal particle size. However, the increase ratio of the adsorption capacities is not along the trend determined by  $CO_2$  (273 K) micropore analyses, which may be attributed to the pulverization-generated SSA and the pore volume whose diameter is less than 10 nm; these space may also contribute to the adsorption capacities. In addition, from the methane desorption curves, the phenomenon that dividing the whole desorption stage into the rapid desorption stage and the normal or slow desorption stage can be obviously recognized, which indicates the existence of coal rank-dependent extremity particle size, the scale of which may change with the variation of the coal rank.

## AUTHOR INFORMATION

### Corresponding Author

\*E-mail: [381zhao@sina.com](mailto:381zhao@sina.com). Tel: +86 516 83885948. Fax: +86 516 83995097.

### ORCID

Yuanping Cheng: [0000-0003-1511-9891](https://orcid.org/0000-0003-1511-9891)

### Notes

The authors declare no competing financial interest.

## ACKNOWLEDGMENTS

The authors are grateful to the National Science Foundation of China (51374204, 51574229, and 51304188), Natural Science Foundation of Jiangsu Province (BK20160253), the financial support from the Project Funded by the Priority Academic Program Development of Jiangsu Higher Education Institutions (PAPD), the Basic Research Program of Jiangsu Province (BK20140206), and the sponsorship of Jiangsu Overseas Research & Training Program for University Prominent Young & Middle-aged Teachers and Presidents.

## REFERENCES

- (1) Wang, F.; Cheng, Y.; Lu, S.; Jin, K.; Zhao, W. Influence of coalification on the pore characteristics of middle–high rank coal. *Energy Fuels* **2014**, *28* (9), 5729–5736.
- (2) Nie, B.; Liu, X.; Yang, L.; Meng, J.; Li, X. Pore structure characterization of different rank coals using gas adsorption and scanning electron microscopy. *Fuel* **2015**, *158*, 908–917.
- (3) Clarkson, C. R.; Bustin, R. M. Variation in micropore capacity and size distribution with composition in bituminous coal of the Western Canadian Sedimentary Basin: Implications for coalbed methane potential. *Fuel* **1996**, *75* (13), 1483–1498.
- (4) Yao, Y.; Liu, D.; Tang, D.; Tang, S.; Huang, W. Fractal characterization of adsorption-pores of coals from North China: an investigation on CH<sub>4</sub> adsorption capacity of coals. *Int. J. Coal Geol.* **2008**, *73* (1), 27–42.
- (5) Pan, Z.; Connell, L. D. Modelling permeability for coal reservoirs: a review of analytical models and testing data. *Int. J. Coal Geol.* **2012**, *92*, 1–44.
- (6) Bustin, R.; Clarkson, C. Geological controls on coalbed methane reservoir capacity and gas content. *Int. J. Coal Geol.* **1998**, *38* (1), 3–26.
- (7) Li, G. Coal reservoir characteristics and their controlling factors in the eastern Ordos basin in China. *Int. J. Min. Sci. Technol.* **2016**, *26* (6), 1051–1058.
- (8) Laubach, S.; Marrett, R.; Olson, J.; Scott, A. Characteristics and origins of coal cleat: a review. *Int. J. Coal Geol.* **1998**, *35* (1), 175–207.
- (9) Lu, S.; Cheng, Y.; Qin, L.; Li, W.; Zhou, H.; Guo, H. Gas desorption characteristics of the high-rank intact coal and fractured coal. *Int. J. Min. Sci. Technol.* **2015**, *25* (5), 819–825.
- (10) Huang, B.; Cheng, Q.; Chen, S. Phenomenon of methane driven caused by hydraulic fracturing in methane-bearing coal seams. *Int. J. Min. Sci. Technol.* **2016**, *26* (5), 919–927.
- (11) Jiang, B.; Qu, Z.; Wang, G. G.; Li, M. Effects of structural deformation on formation of coalbed methane reservoirs in Huaibei coalfield, China. *Int. J. Coal Geol.* **2010**, *82* (3), 175–183.
- (12) Lu, S.-q.; Cheng, Y.-p.; Li, W.; Wang, L. Pore structure and its impact on CH<sub>4</sub> adsorption capability and diffusion characteristics of normal and deformed coals from Qinshui Basin. *Int. J. Oil, Gas Coal Technol.* **2015**, *10* (1), 94–114.
- (13) Lu, S.; Cheng, Y.; Ma, J.; Zhang, Y. Application of in-seam directional drilling technology for gas drainage with benefits to gas outburst control and greenhouse gas reductions in Daning coal mine, China. *Natural Hazards* **2014**, *73* (3), 1419–1437.
- (14) Jian, K.; Lei, D.; Fu, X.; Zhang, Y.; Li, H. Effect of an electrostatic field on gas adsorption and diffusion in tectonic coal. *Int. J. Min. Sci. Technol.* **2015**, *25* (4), 607–613.
- (15) Airey, E. Gas emission from broken coal. An experimental and theoretical investigation. *International Journal of Rock Mechanics and Mining Sciences & Geomechanics Abstracts*; Elsevier: Amsterdam, 1968; pp 475–494.
- (16) Bertard, C.; Bruyet, B.; Gunther, J. In Determination of desorbable gas concentration of coal (direct method). *International Journal of Rock Mechanics and Mining Sciences & Geomechanics Abstracts*, 1970; Elsevier: Amsterdam, 1970; pp 43–65.
- (17) Bielicki, R. J.; Perkins, J. H.; Kissell, F. N. *Methane diffusion parameters for sized coal particles: A measuring apparatus and some preliminary results*; Bureau of Mines: Washington, DC, 1972.
- (18) Nandi, S. P.; Walker, P. L. Activated diffusion of methane from coals at elevated pressures. *Fuel* **1975**, *54* (2), 81–86.
- (19) Clarkson, C.; Bustin, R. The effect of pore structure and gas pressure upon the transport properties of coal: a laboratory and modeling study. 1. Isotherms and pore volume distributions. *Fuel* **1999**, *78* (11), 1333–1344.
- (20) Clarkson, C.; Bustin, R. The effect of pore structure and gas pressure upon the transport properties of coal: a laboratory and modeling study. 2. Adsorption rate modeling. *Fuel* **1999**, *78* (11), 1345–1362.
- (21) Wang, G.; Wang, K.; Ren, T. Improved analytic methods for coal surface area and pore size distribution determination using 77K nitrogen adsorption experiment. *Int. J. Min. Sci. Technol.* **2014**, *24* (3), 329–334.

- (22) Yao, Y.; Liu, D.; Tang, D.; Tang, S.; Huang, W.; Liu, Z.; Che, Y. Fractal characterization of seepage-pores of coals from China: an investigation on permeability of coals. *Comput. Geosci.* **2009**, *35* (6), 1159–1166.
- (23) Cai, Y.; Liu, D.; Pan, Z.; Yao, Y.; Li, J.; Qiu, Y. Pore structure and its impact on CH<sub>4</sub> adsorption capacity and flow capability of bituminous and subbituminous coals from Northeast China. *Fuel* **2013**, *103*, 258–268.
- (24) Crosdale, P. J.; Beamish, B. B.; Valix, M. Coalbed methane sorption related to coal composition. *Int. J. Coal Geol.* **1998**, *35* (1–4), 147–158.
- (25) An, F.-H.; Cheng, Y.-P.; Wu, D.-M.; Wang, L. The effect of small micropores on methane adsorption of coals from Northern China. *Adsorption* **2013**, *19* (1), 83–90.
- (26) Jiang, H.; Cheng, Y.; Yuan, L. A Langmuir-like desorption model for reflecting the inhomogeneous pore structure of coal and its experimental verification. *RSC Adv.* **2015**, *5* (4), 2434–2440.
- (27) Gürdal, G.; Yalçın, M. N. Pore volume and surface area of the Carboniferous coals from the Zonguldak basin (NW Turkey) and their variations with rank and maceral composition. *Int. J. Coal Geol.* **2001**, *48* (1), 133–144.
- (28) Lutynski, M.; González González, M. Á. Characteristics of carbon dioxide sorption in coal and gas shale – The effect of particle size. *J. Nat. Gas Sci. Eng.* **2016**, *28*, 558–565.
- (29) Karacan, C. Ö.; Mitchell, G. D. Behavior and effect of different coal microlithotypes during gas transport for carbon dioxide sequestration into coal seams. *Int. J. Coal Geol.* **2003**, *53* (4), 201–217.
- (30) Azmi, A. S.; Yusup, S.; Muhamad, S. The influence of temperature on adsorption capacity of Malaysian coal. *Chem. Eng. Process.* **2006**, *45* (5), 392–396.
- (31) Slezak, A.; Kuhlman, J. M.; Shadle, L. J.; Spenik, J.; Shi, S. CFD simulation of entrained-flow coal gasification: Coal particle density/sizefraction effects. *Powder Technol.* **2010**, *203* (1), 98–108.
- (32) Yu, D.; Xu, M.; Sui, J.; Liu, X.; Yu, Y.; Cao, Q. Effect of coal particle size on the proximate composition and combustion properties. *Thermochim. Acta* **2005**, *439* (1), 103–109.
- (33) Versan Kök, M.; Özbas, E.; Karacan, O.; Hicyilmaz, C. Effect of particle size on coal pyrolysis. *J. Anal. Appl. Pyrolysis* **1998**, *45* (2), 103–110.
- (34) Gore, R.; Crowe, C. T. Effect of particle size on modulating turbulent intensity. *Int. J. Multiphase Flow* **1989**, *15* (2), 279–285.
- (35) Zhao, W.; Cheng, Y.; Jiang, H.; Jin, K.; Wang, H.; Wang, L. Role of the rapid gas desorption of coal powders in the development stage of outbursts. *J. Nat. Gas Sci. Eng.* **2016**, *28*, 491–501.
- (36) Zhong, S.; Baitalow, F.; Nikrityuk, P.; Gutte, H.; Meyer, B. The effect of particle size on the strength parameters of German brown coal and its chars. *Fuel* **2014**, *125*, 200–205.
- (37) Brunauer, S.; Emmett, P. H.; Teller, E. Adsorption of gases in multimolecular layers. *J. Am. Chem. Soc.* **1938**, *60* (2), 309–319.
- (38) Barrett, E. P.; Joyner, L. G.; Halenda, P. P. The determination of pore volume and area distributions in porous substances. I. Computations from nitrogen isotherms. *J. Am. Chem. Soc.* **1951**, *73* (1), 373–380.
- (39) Lowell, S.; Shields, J. E.; Thomas, M. A.; Thommes, M. *Characterization of porous solids and powders: Surface area, pore size and density*; Springer Science & Business Media: Dordrecht, 2012; Vol. 16.
- (40) Landers, J.; Gor, G. Y.; Neimark, A. V. Density functional theory methods for characterization of porous materials. *Colloids Surf., A* **2013**, *437*, 3–32.
- (41) Sing, K. Reporting physisorption data for gas/solid systems with special reference to the determination of surface area and porosity (Provisional). *Pure Appl. Chem.* **1982**, *54* (11), 2201–2218.
- (42) Soave, G. Equilibrium constants from a modified Redlich-Kwong equation of state. *Chem. Eng. Sci.* **1972**, *27* (6), 1197–1203.
- (43) Laxminarayana, C.; Crosdale, P. J. Role of coal type and rank on methane sorption characteristics of Bowen Basin, Australia coals. *Int. J. Coal Geol.* **1999**, *40* (4), 309–325.
- (44) Cecil, C. B.; Stanton, R.; Dulong, F.; Renton, J. Geologic factors that control mineral matter in coal. In *Atomic and Nuclear Methods in Fossil Energy Research*; Springer: Boston, 1982; pp 323–335.
- (45) Cloke, M.; Lester, E.; Belghazi, A. Characterisation of the properties of size fractions from ten world coals and their chars produced in a drop-tube furnace. *Fuel* **2002**, *81* (5), 699–708.
- (46) Jin, K.; Cheng, Y.; Wang, L.; Dong, J.; Guo, P.; An, F.; Jiang, L. The effect of sedimentary redbeds on coalbed methane occurrence in the Xutuan and Zhaoji Coal Mines, Huaibei Coalfield, China. *Int. J. Coal Geol.* **2015**, *137*, 111–123.
- (47) Chen, S.; Zhu, Y.; Li, W.; Wang, H. Influence of magma intrusion on gas outburst in a low rank coal mine. *Int. J. Min. Sci. Technol.* **2012**, *22* (2), 259–266.
- (48) Thommes, M.; Cychosz, K. A. Physical adsorption characterization of nanoporous materials: progress and challenges. *Adsorption* **2014**, *20* (2–3), 233–250.
- (49) Thommes, M.; Kaneko, K.; Neimark, A. V.; Olivier, J. P.; Rodriguez-Reinoso, F.; Rouquerol, J.; Sing, K. S. Physisorption of gases, with special reference to the evaluation of surface area and pore size distribution (IUPAC Technical Report). *Pure Appl. Chem.* **2015**, *87* (9–10), 1051–1069.
- (50) Li, X.; Wang, Z.; Guo, M.; Zhang, J.; Qi, S.; Zhou, B.; Zhang, W. Pore structure characteristics of the Lower Paleozoic formation shale gas reservoir in northern Guizhou. *Journal of China University of Mining & Technology* **2016**, *45* (6), 1156–1167.
- (51) Guo, H.; Cheng, Y.; Wang, L.; Lu, S.; Jin, K. Experimental study on the effect of moisture on low-rank coal adsorption characteristics. *J. Nat. Gas Sci. Eng.* **2015**, *24*, 245–251.
- (52) Pyun, S.-I.; Rhee, C.-K. An investigation of fractal characteristics of mesoporous carbon electrodes with various pore structures. *Electrochim. Acta* **2004**, *49* (24), 4171–4180.
- (53) De Boer, J.; Everett, D.; Stone, F. *The structure and properties of porous materials*; Butterworths: London, 1958.
- (54) Thommes, M. Physical Adsorption Characterization of Nanoporous Materials. *Chem. Ing. Tech.* **2010**, *82* (7), 1059–1073.
- (55) Mastalerz, M.; He, L.; Melnichenko, Y. B.; Rupp, J. A. Porosity of coal and shale: insights from gas adsorption and SANS/USANS techniques. *Energy Fuels* **2012**, *26* (8), 5109–5120.
- (56) Mitropoulos, A. C.; Stefanopoulos, K.; Kanellopoulos, N. Coal studies by small angle X-ray scattering. *Microporous Mesoporous Mater.* **1998**, *24* (1), 29–39.
- (57) Mastalerz, M.; Solano-Acosta, W.; Schimmelmann, A.; Drobnik, A. Effects of coal storage in air on physical and chemical properties of coal and on gas adsorption. *Int. J. Coal Geol.* **2009**, *79* (4), 167–174.
- (58) Yu, Q.; Cheng, Y. *Coal Mine Gas Control*; China University of Mining and Technology Press: Xuzhou, 2012.
- (59) Cheng, Y.; Wang, H.; Wang, L.; Zhou, H.; Liu, H.; Wu, D.; Li, W. *Theories and Engineering Applications on Coal Mine Gas Control*; China University of Mining and Technology Press: Xuzhou, 2010.
- (60) Groen, J. C.; Peffer, L. A.; Pérez-Ramírez, J. Pore size determination in modified micro- and mesoporous materials. Pitfalls and limitations in gas adsorption data analysis. *Microporous Mesoporous Mater.* **2003**, *60* (1), 1–17.
- (61) Gor, G. Y.; Thommes, M.; Cychosz, K. A.; Neimark, A. V. Quenched solid density functional theory method for characterization of mesoporous carbons by nitrogen adsorption. *Carbon* **2012**, *50* (4), 1583–1590.
- (62) Neimark, A. V.; Lin, Y.; Ravikovitch, P. I.; Thommes, M. Quenched solid density functional theory and pore size analysis of micro-mesoporous carbons. *Carbon* **2009**, *47* (7), 1617–1628.
- (63) Busch, A.; Gensterblum, Y.; Krooss, B. M.; Littke, R. Methane and carbon dioxide adsorption–diffusion experiments on coal: upscaling and modeling. *Int. J. Coal Geol.* **2004**, *60* (2), 151–168.
- (64) Li, Y. H.; Lu, G. Q.; Rudolph, V. Compressibility and fractal dimension of fine coal particles in relation to pore structure characterisation using mercury porosimetry. *Part. Part. Syst. Charact.* **1999**, *16* (1), 25–31.

- (65) Amarasekera, G.; Scarlett, M. J.; Mainwaring, D. E. Micropore size distributions and specific interactions in coals. *Fuel* **1995**, *74* (1), 115–118.
- (66) Mathews, J. P.; Hatcher, P. G.; Scaroni, A. W. Particle size dependence of coal volatile matter: is there a non-maceral-related effect? *Fuel* **1997**, *76* (4), 359–362.
- (67) Pillalamarri, M.; Harpalani, S.; Liu, S. Gas diffusion behavior of coal and its impact on production from coalbed methane reservoirs. *Int. J. Coal Geol.* **2011**, *86* (4), 342–348.
- (68) Harpalani, S.; Prusty, B. K.; Dutta, P. Methane/CO<sub>2</sub> sorption modeling for coalbed methane production and CO<sub>2</sub> sequestration. *Energy Fuels* **2006**, *20* (4), 1591–1599.
- (69) Sudibandriyo, M.; Pan, Z.; Fitzgerald, J. E.; Robinson, R. L.; Gasem, K. A. Adsorption of methane, nitrogen, carbon dioxide, and their binary mixtures on dry activated carbon at 318.2 K and pressures up to 13.6 MPa. *Langmuir* **2003**, *19* (13), 5323–5331.
- (70) Langmuir, I. The adsorption of gases on plane surfaces of glass, mica and platinum. *J. Am. Chem. Soc.* **1918**, *40* (9), 1361–1403.
- (71) Joubert, J. I.; Grein, C. T.; Bienstock, D. Sorption of methane in moist coal. *Fuel* **1973**, *52* (3), 181–185.
- (72) Zhao, W.; Cheng, Y.; Yuan, M.; An, F. Effect of Adsorption Contact Time on Coking Coal Particle Desorption Characteristics. *Energy Fuels* **2014**, *28* (4), 2287–2296.
- (73) Hodot, B. B. *Outburst of Coal and Coalbed Gas*. China Industry Press: Beijing, 1966.
- (74) Harpalani, S.; Chen, G. Influence of gas production induced volumetric strain on permeability of coal. *Geotech. Geol. Eng.* **1997**, *15* (4), 303–325.
- (75) King, G. Numerical simulation of the simultaneous flow of methane and water through dual porosity coal seams during the degasification process. Ph.D. Thesis, Pennsylvania State University, University Park, PA, 1984.
- (76) Zhou, S. Mechanism of gas flow in coal seams. *Journal of China Coal Society* **1990**, *15* (1), 15–24.
- (77) Li, H.; Lin, B.; Yang, W.; Zheng, C.; Hong, Y.; Gao, Y.; Liu, T.; Wu, S. Experimental study on the petrophysical variation of different rank coals with microwave treatment. *Int. J. Coal Geol.* **2016**, *154–155*, 82–91.
- (78) Lu, X.; Liu, Z.; Liu, J.; Lu, C.; Li, T.; Sun, D. Research on the dynamic evaluation method for oil-bearing degree of low-permeability and tight sandstone reservoirs: a case from the Yanchang formation of south Ordos basin. *Journal of China University of Mining & Technology* **2016**, *45* (6), 1118–1128.
- (79) Zhao, Y.; Liu, S.; Elsworth, D.; Jiang, Y.; Zhu, J. Pore structure characterization of coal by synchrotron small-angle X-ray scattering and transmission electron microscopy. *Energy Fuels* **2014**, *28* (6), 3704–3711.
- (80) Rouquerol, J.; Baron, G. V.; Denoyel, R.; Giesche, H.; Groen, J.; Klobes, P.; Levitz, P.; Neimark, A. V.; Rigby, S.; Skudas, R.; et al. The characterization of macroporous solids: an overview of the methodology. *Microporous Mesoporous Mater.* **2012**, *154*, 2–6.
- (81) Ottiger, S.; Pini, R.; Storti, G.; Mazzotti, M. Competitive adsorption equilibria of CO<sub>2</sub> and CH<sub>4</sub> on a dry coal. *Adsorption* **2008**, *14* (4–5), 539–556.